AN ANGSA STUDY OF ILMENITE CRYSTAL SIZE DISTRIBUTIONS OF BASALT CLASTS IN DRIVE TUBE 73002 J. L. Valenciano[1], C. R. Neal[1], C. K. Shearer[2], and the ANGSA Science Team, [1]Department of Civil and Environmental Engineering and Earth Sciences, University of Notre Dame, Notre Dame, IN 46556, USA [2]Institute of Meteoritics, University of New Mexico, Albuquerque, NM, USA (jvalenc2@nd.edu; cneal@nd.edu; cshearer@unm.edu)

Introduction: During Apollo 17, two vacuum-sealed drive tubes were collected at Station 3 that formed samples 73001 (lower) and 73002 (upper) (**Fig. 1**) [1]. These samples are part of the Apollo Next Generation Sample Analysis (ANGSA) project, which seeks to use these samples as part of educating the next generation of lunar sample scientists and offer new perspectives on solar wind and lunar volatiles, as well as potentially discovering new lithologies from a landslide deposit that Station 3 sampled. Drive tube 73002 has been imaged using x-ray computerized tomography (XCT), and from those images nine basalt clasts (,27G-C1; ,27G-C2; ,51A; ,51C; ,80A; ,1095A; ,1121A; ,1141A and ,2015) were identified (**Fig. 2**). The XCT images were used to investigate the crystallization history of these clasts by constructing ilmenite crystal size distributions (CSD).

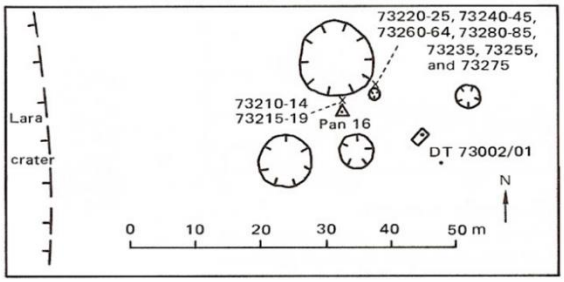

Figure 1: Schematic showing the location of drive tube 73002 in relation to other station 3 samples [1].

Methods: CSDs are a quantitative method of analyzing the crystallization processes that sample experienced. CSDs are based on the principle that the crystal size and the natural log of the number of crystals existing in individual size intervals have a linear, negative correlation and that the slope of the CSD can be used to calculate residence times (if the growth rate is known), as well as the relationship between nucleation and the growth rate [2,3]. The data collected for this study uses a process similar to that described in [4]. Several user-selected "slices" from the CT scan were taken throughout each clast

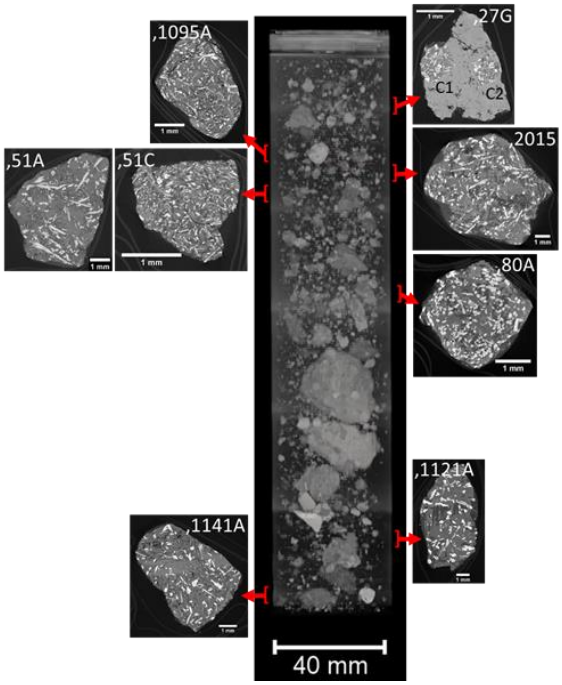

Figure 2: XCT scans of the basalt clasts analyzed in this study and their approximate location within 73002. Breccia fragment ,27G contained two basalt clasts, which were split into clast 1 (C1) and clast 2 (C2) and analyzed separately.

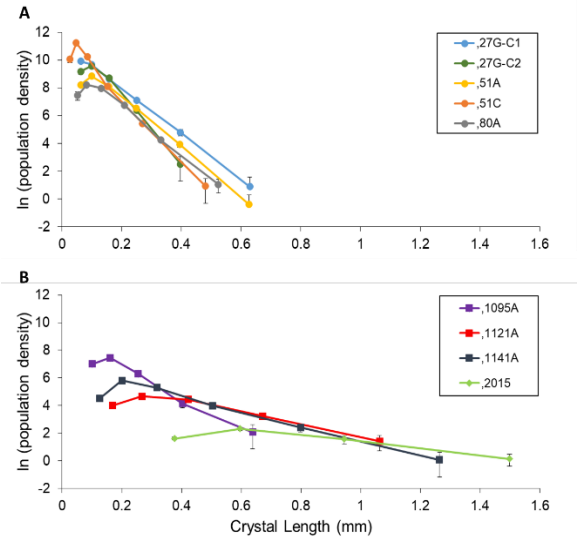

Figure 3: CSD profiles of (A) clasts from Pass 1 and (B) clasts from Passes 2 and 3. If error bars are not visible, they are within the symbol.

and then imported into *Corel Paintshop Pro 2020*. Individual ilmenite crystals were then identified and traced using a touch-screen laptop computer and an active stylus pen. Any crystals that shared a boundary were traced on separate layers and any crystals located on the edges of the clasts were not included in the analysis because they were not complete. A minimum of 250 crystals is necessary to generate a statistically meaningful population density for inequant crystals [5], and for this study between 300 – 1800 ilmenite crystals were traced for each clast. Armacolite is present in ,51A and was included as ilmenite for this study. The resulting crystal traces were then filled in with a solid color and imported to *ImageJ*, where the area, best-fit ellipse, and major and minor axis of each crystal were calculated using the known scale of each clast. The major and minor axes data is exported to *CSDSlice* and compared to a database of >700 crystals in order to determine the best shape of each 2-D crystal tracing [5]. *CSDCorrections* was then used to group crystal sizes into bins and plot the natural log of the population density against the major axis length of each crystal [6] (**Fig. 3**).

Results and Discussion: Each of the basalt clasts analyzed show linear CSDs, which is indicative of a constant cooling rate. The steeper slopes of some clasts (**Fig. 3A**) demonstrate a faster cooling rate compared to the shallower slopes of others that cooled less rapidly (**Fig. 3B**), which is supported by the larger crystals present in clasts with shallow slopes. The different CSD types could be an indication that these clasts were from different flows or represent different areas of the same flow. It is possible that the samples represented by a faster cooling rate were from the edge of the flow and the slower cooling rates originate from the interior of the flow, however, this is not able to be confirmed due to the absence of compositional data. When compared with other high-Ti basalts that have been analyzed two populations can be seen (**Fig. 4**). The clasts with steeper slopes (,27G-C1; ,27G-C2; ,51A; ,51C; ,80A; ,1095A) follow the upper "faster' cooling trend while the remained shallower-sloped clasts (,1121A; ,1141A; ,2015) plot within the "slower" cooling trend.

The textures these clasts were then compared to those in [7,8] to provide an estimation of their cooling rates. Based on the similarity of their textures, the 6 clasts plotting on the "faster" cooling trend crystallized at a rate of 2-7˚C/hr, whereas the 3 clasts plotting on the "slower" cooling trend cystallized at a rate of <1˚C/hr. Future work is needed to undertake controlled cooling rate experiments and conduct ilmenite CSDs on the products to properly quantify the cooling rates that are represent on diagr include cooling experiments carried out in terms of ilmenite, from which CSDs will also be constructed and then compared to those presented in this study.

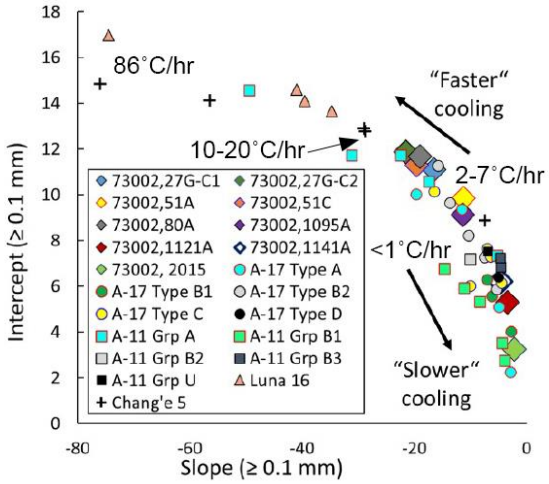

Figure 4: Comparison of ilmenite CSD slopes and intercepts of the 73002 basalts from this study and previously studied Apollo 11 and 17 high-Ti basalts. Cooling rates estimated from [7,8]

Acknowledgements: We thank the ANGSA Preliminary Examination Team and the curatorial staff at JSC for their work and for allocating the samples, and NASA for supporting ANGSA. This was supported by NASA Grant 80NSSC19K1099 to CKS and the subcontract to the University of Notre Dame.

References: [1] Wolfe, E.W. et. al. (1981) *USGS Professional Paper*, 1080. [2] Marsh, B.D., (1998) *J Petrol 39 (4)*, 553-599. [3] Cashman, K.V. & Marsh, B.D. (1988) *CMP 99 (3)*, 292-305. [4] Neal et. al. (2015) *GCA 146*, 62-80. [5] Morgan D. J., & Jerram D.A. (2006) *JVGR 154*, 1-7. [6] Higgins M. D. (2000) *Amer. Min. 85*, 1105-1116 [7] Usselman T. M. et al. (1975) PLSC 6, 997-1020; [8] Usselman T. M. & Lofgren G. E., (1976) *PLSC 7*, 1345-1363.